Indian Journal of Chemical Technology
Vol. 33, July 2026, pp. 628-638
DOI: 10.56042/ijct.v33i4.25516

Development and characterization of nanocellulose hydrogel for enhanced water retention and controlled nutrient release in sustainable agriculture

Jamesraj Sathish[1], Ramasamy Palani[2]* & Muthulingam Seenuvasan[3]

[1]Department of Chemical Engineering, KPR Institute of Engineering and Technology, Coimbatore, Tamil Nadu, India

[2]Department of Chemical Engineering, Hindusthan College of Engineering and Technology, Coimbatore, Tamil Nadu, India

[3]Department of Education, National Institute of Technical Teachers Training and Research, Chennai, Tamil Nadu, India

*E-mail: palani79@gmail.com

Received 12 November 2025; Accepted 9 April 2026

This work presents the synthesis and characterization of a coconut shell waste-derived nanocellulose-based hydrogel for green agriculture. The hydrogel was designed to enhance water retention of soil and deliver controlled release of nutrients, addressing the major problems of drought and fertilizer inefficiency. Nanocellulose was prepared through acid hydrolysis after alkaline and bleaching treatment and cross-linked with citric acid to yield a urea-loaded hydrogel. Fourier Transform Infrared spectra verified the integrity of cellulose functional groups and the formation of new $–COO^-$ bonds, evidencing good crosslinking and urea incorporation. X-ray diffractogram evidenced prominent crystalline peaks at $2\theta \approx 15°$ and 22.5°, signifying partial retention of cellulose I structure with reduced crystallinity, augmenting swelling and water-retention capacity. Scanning Electron Microscope images exhibited a sharp, porous, and networked structure that supports water uptake, nutrient transfer, and mechanical strength. Hydrogel exhibited a 50% increase in water retention and an 88% degree of nutrient release efficiency, greatly supporting soil parameters such as nitrogen level and water content. Soil analysis after treatment showed high ammoniacal nitrogen (7.6 mg/kg) and a notable rise in total Kjeldahl nitrogen (13.1%), confirming efficacy of nutrient delivery. These results set the hydrogel's dual function as a moisture regulator and slow-release fertilizer system. Overall, the nanocellulose hydrogel derived from coconut shells is an economically scaled, biodegradable, and environmentally friendly material for smart agriculture with benefits towards water conservation, reduced fertilizer loss, and climate-stressed crop productivity in a sustainable way.

Keywords: Coconut shell cellulose, Controlled nutrient release, Nano-cellulose hydrogel, Sustainable agriculture Water retention

Introduction

Climate change and continuous freshwater shortages are significant challenges for agriculture around the globe. Hence, finding new solutions to address new issues is as important as improving use of existing resources, and consequently, crop productivity[1]. With estimates indicating that the world's population could reach 9.7 billion by 2050, we must leverage technologies that improve the soil's ability to hold water and obtain nutrients with little additional environmental impact[2]. Various materials have been examined, including hydrogels. Hydrogels are 3D polymer networks capable of storing large quantities of water that can be made available for plant roots[3,4]. Recent studies have highlighted the potential of nanocellulose-based hydrogels for sustainable agricultural applications due to their high surface area, biodegradability, and excellent water absorption capacity. Hydrogels derived from cellulose nanofibers and nanocrystals obtained from agricultural residues such as wheat straw and jute fibers have shown improved soil moisture retention and nutrient use efficiency under controlled conditions[4-6] . Hydrogels based on natural polymers that are obtained from a renewable biomass generated the most interest. They are biocompatible, can decompose, and are renewable. There is abundant plant-based biomass in agricultural wastes that are commonly not used or simply discarded[7]. These offer an opportunity for more sustainable resources management and sustainable use. The coconut shell waste is particularly interested in this regard. It is simple to obtain, inexpensive, and is a good substrate for cellulose extraction. Cold tropical and subtropical regions generate millions of tons of coconut shell waste on a yearly basis, and disposal creates challenges[5,8]. The ability to utilize coconut waste to generate useful products such as nanocellulosic products fits within the concepts of a circle economy and sustainability[6]. Several pre-treatments are needed to remove lignin and

hemicelluloses in order to get cellulose from coconut shells. Then chemical treatments like alkali and acid hydrolysis are used to separate the cellulose fibers[9] followed by mechanical or chemical processes such as sulfuric acid hydrolysis to shrink these cellulose fibers to the nanoscale to prepare cellulose nanocrystals or cellulose nanofibers[10,11]. These nanocellulose materials have amazing qualities, including a large surface area great strength changeable surface chemistry, and the ability to break down[12]. This makes them perfect for many different uses. The special features of nanocellulose how it can form stable three-dimensional networks, make it good for creating hydrogels. When nanocellulose is added to hydrogels, it can improve how much water they hold how strong they are, and how well they can control the release of things inside them[13]. However, several limitations remain in existing systems.

Many reported hydrogels involve complex synthesis methods, non-biodegradable additives, or lack validation under real soil conditions. In addition, limited research has focused on utilizing low-cost agro-waste such as coconut shells for nanocellulose extraction. Most studies also evaluate either water retention or nutrient release separately, without integrating both functions into a single system[13,14]. These nanocellulose-based hydrogels offer a green and effective way to improve farming by acting as smart systems to deliver water and nutrients to soil[15]. By boosting how much water they can hold, these hydrogels cut down on how often you need to water, which saves fresh water[16,17]. At the same time, they let out nutrients, which means crops use nutrients better and less fertilizer runs off into the environment causing less pollution[18]. The global market for slow-release fertilizers was worth ₹20,969 crore in 2024 and is set to grow ₹27,958 crore by 2029. Regular fertilizers often leak or evaporate, with crops taking up 30-50% of nitrogen and 10-45% of phosphorus. Adding nanocellulose to hydrogels can reduce these losses by releasing nutrients over time and making soil structure and moisture better[19]. Moreover, there are no studies on the environmental implications of nanoparticle residues or their reproducibility in terms of structure and function[20].

To address these gaps, the present study focuses on the development of a nanocellulose-based hydrogel derived from coconut shell waste using an environmentally friendly and scalable synthesis approach. The specific objectives of this work are to extract nanocellulose through chemical treatment methods, to synthesize a citric acid crosslinked and urea-loaded hydrogel system, and to characterize its structural and morphological properties using Fourier transform infrared spectroscopy (FTIR), X-ray diffraction (XRD), and scanning electron microscopy (SEM) techniques. In addition, the study evaluates the functional performance of the hydrogel in terms of water retention capacity and controlled nutrient release in soil conditions. By integrating waste valorization with advanced material design, this work aims to provide a sustainable solution for improving soil moisture management and fertilizer efficiency, contributing to climate-resilient agricultural practices.

Experimental Section

Cellulose preparation

A systematic procedure for the preparation of cellulose from coconut shell was initiated, including cleaning, chemical modification, and purification step. Initially, 1000 g of fully matured and dry coconut shells was collected, washed with water to remove all dust and surface impurities, and oven dried at 60–70 °C for 24 h. The dried shells underwent mechanical grinding and were sieved until homogeneous particle size was obtained. The powdered coconut shell was subjected to an alkaline treatment for the removal of lignin and hemicellulose, the powdered coconut shell was treated in sodium hydroxide (NaOH) the solution (4–10% w/v) was made with a solid to liquid ratio of 1:10 and mixed while heating at 80–90 °C for 2 to 3 h. After reaction the mixture was filtered, cooled, then the solid product was washed several times with distilled water until neutral pH was obtained. Bleaching of cellulose is performed on the delignified material to remove residual lignin and further purify the cellulose[12,19]. Then it added glacial acetic acid was to make an acidified 1.5% sodium chlorite ($NaClO_2$) solution in the pH range of 4 to 5. The residue was added to this solution and heated at between 70–80 °C for 1 to 2 h. After the treatment, the solid was filtered, and then thoroughly washed with distilled water to neutralize the pH. The purified cellulose was washed, dried at 60 °C, and stored for further use.

Nano-cellulose preparation

A sodium hydroxide treatment where cellulose (700 g) was treated with a sodium hydroxide solution at 80 °C and washed, and then bleached in hydrogen

peroxide at 70 °C to eliminate any residual colours. Once the cellulose was purified and then washed to a neutral pH and dried, the core of the study was acid hydrolysis.This was done in a fume hood with proper safety precautions. Dry cellulose was combined with a 64% solution of sulfuric acid and was heated at 50 °C for 45 min. We stopped the reaction by diluting the acidic mixture with a lot of cold distilled water. The last purification required rinsing the product in succession, centrifuging the nanocellulose, and rinsing until we reached a pH of neutrality. The dialyzed suspension for two days until it was of pure character. A final step with sonication to disintegrate any lumps yielded a stable gel-phase suspension of nanocellulose[9].

Urea-loaded nanocellulose hydrogel preparation

To start, 550 g of nanocellulose suspension was placed in a beaker. The mixture was then added with citric acid at 10% by weight of cellulose. Citric acid was used as the cross-linking agent, followed by the addition of 100 g of urea. The mixture was stirred with a magnetic stirrer until the citric acid and urea were well distributed in the suspension. The even blend was transferred into a petri dish, which served as a mold. The mold was then put into an oven at 80 °C for 3 h. Here, the citric acid began to form cross-links between the nanocellulose fibers. As curing, the liquid suspension evolved into a firm and flexible hydrogel.After curing, the hydrogel was removed from the oven and cooled to room temperature. To stabilize the product, the hydrogel was washed by submerging it in deionized water and gently agitating. This process eliminated any unreacted citric acid or loosely associated urea on the surface. The final result was a stable, solid, urea-loaded nanocellulose hydrogel. This hydrogel has been used to develop three different slow-releasing fertilizer products[5,13].

Slow release fertilizer powder preparation

To prepare urea-loaded nanocellulose hydrogel (200 g) for drying, the block was cut into thin slices (10 mm thick), to increase the surface area and promote uniform moisture removal. The hydrogel sheets were laid out on a sterilized tray and placed in a hot air oven. The gel dried out at a steady temperature of 60 °C for 24 h. At the end of the drying cycle, the weight change in the material had stopped indicating it had been completely dried of moisture. The dried material was a solid, hard and brittle product with much less weight. After cooling the dried material all the way down to room temperature, the material was transferred into a ceramic mortar and pestle. The dried size was then carefully crushed into a fine powder[20]. The powder then underwent a sieving process to ensure a consistent particle size. The sieved product, selected as the final product, was the granular fraction between the 0.7 mm and 0.5 mm mesh sieve. This size fraction was determined to be most appropriate for application into soil. This was done to create a slow release fertilizer powder. The steps for preparation are shown in Fig. 1.

Slow release soil amendment chunks

To prepare urea-loaded nanocellulose hydrogel (175 g), was sliced into small uniform cubes (20 mm thick), to increase the surface area and promote uniform moisture removal. These chunks are then mixed directly into soil. Adding chunks acts as a soil amendment to improve water retention and provides steady supply of slow release nutrients as it biodegrades[21].

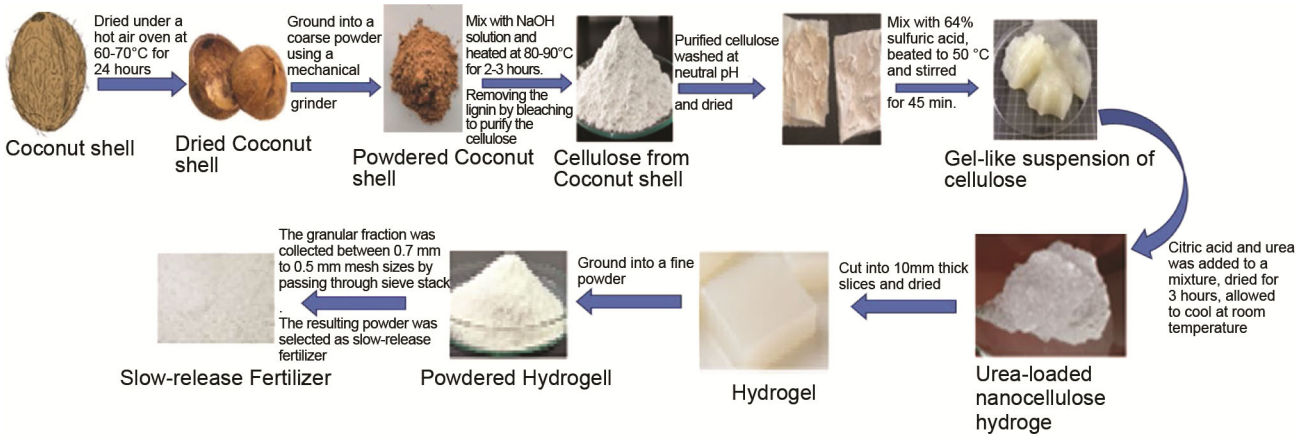

Fig. 1 — Schematic for the preparation of slow release fertilizer powder

Slow release seedling starter blocks

To prepare urea-loaded nanocellulose hydrogel (175 g), was sliced into small uniform blocks (20 mm thick) and single seeds were inserted into the center of each cubes. This hydrogel block acts as a self-contained, biodegradable starter pot that provides the germinating seed with all the water and nutrients[22]. The entire block is planted directly into the soil and it releases nutrients as it biodegrades over time.

Soil test parameters and relevance to hydrogel application

It is essential to understand the current state of the soil, for instance pH, nitrogen, organic matter, microbial activity, before utilization of cellulose-based hydrogel. The baseline data (obtained from soil testing) will show the soil condition and aide to monitor the effectiveness of the hydrogel over time. Soil testing is the analysis of chemical, physical, and biological propertiesof the soil. It is necessary to know the soil suitability for different agricultural purposes (such as crop, and ultimately food, production). Hydrogels reduce plant water stress and decrease the need for frequent irrigation in areas with irrigation systems through their water-retention abilities and nutrient-holding characteristics. Soil testing consists of essential stages which begin with gathering representative soil samples followed by appropriate sample handling and laboratory examination for important parameters and ending with soil type and crop requirement-based interpretation of test results. The process guarantees precise reliable data which supports well-informed decision making.

Cellulose-based hydrogels have a soft, jelly-like texture when they are hydrated because they contain a lot of water. They can be incorporated into soil either in a pre-soaked state or directly in dry form. The pre-soaked method is ideal for smaller areas, while the dry application method is more suitable for large-scale use. To ensure accuracy and consistency, soil test parameters were evaluated in triplicate as shown in Table 1 before the hydrogel was applied to the agricultural field.

Results and Discussion

FTIR analysis cellulose, nanocellulose and hydrogel

Fig. 2(a) shows the FT-IR spectrum obtained for cellulose sample. It showed the broad peak at 3332 cm^{-1} attributed to the -OH stretching of hydroxyl

Table 1 — Soil test parameters before hydrogel application

S. No.	Parameter	Unit	Test Method	Results
1	Water content	%	IS 2720-2[23]	8.86
2	Organic matter	%	IS 2720-22[24]	0.78
3	pH value	-	IS 2720-26[25]	8.36
4	Specific electrical conductivity	µs/cm	IS 14767[26]	480
5	Sulphate	mg/100g	SOP No. Soil/010[27]	48
6	Available phosphorous	µg/g	SOP No. Soil/001[28]	35
7	Soluble calcium and magnesium	meq/L (milliequivalents per liter)	SOP No. Soil/009[29]	1.22
8	Soluble calcium	meq/L	SOP No. Soil/008[30]	1.22
9	Carbonate	meq/L	SOP No. Soil/005[31]	Nil
10	Bicarbonate	meq/L	SOP No. Soil/003[32]	0.18
11	Chloride	meq/L	SOP No. Soil/006[33]	22.1
12	Bulk density	g/cc	SOP No. Soil/004[34]	1.35
13	Pore space	%	SOP No. Soil/007[35]	26
14	Ammoniacal nitrogen	mg/kg	IS 14684:1999[36]	BDL(DL:1.0)
15	Total Kjeldahl nitrogen	%	IS 14684:1999[36]	0.0388
16	Water holding capacity	%	SOP No. Soil/011[37]	50
17	Soil texture	-	FAO Method[38]	Silty loam
18	Sand	%		17.5
19	Silt	%	Robinson Pipette Method[39]	72.8
20	Clay	%		9.7
21	Chemical oxygen demand	mg/kg	Inhouse Method[40]	13447
22	Biochemical oxygen demand (3days @ 27ºC	mg/kg	Inhouse Method[40]	1450
23	Soluble sodium	mg/kg	FAO Method[41]	1025
24	Soluble potassium	mg/kg	FAO Method[42]	88
25	Cation exchange capacity	meq/100 g	FAO Method[43]	16.5

groups. The peak at 2892 cm^{-1} corresponds to the C-H stretching of CH_2 and CH units present in the cellulose structure. The band at 1636 cm^{-1} attributes to the -OH bending vibration of intercalated or adsorbed water molecules in cellulose. Peaks observed between 1427-1200 cm^{-1} correspond to the bending vibrations of CH_2 and CH functionalities of cellulose[44]. C-O-C asymmetric stretching and C-O and C-C stretching vibrations were observed at 1159 cm^{-1}, 1051 and 1029 cm^{-1}. The peak at 894 cm^{-1} is attributed to the β-glycosidic linkage between the two glucose units of cellulose. Hence, IR spectrum of cellulose sample confirmed the presence of characteristics peaks of cellulose and the hydroxyl groups of cellulose can be functionalized to prepare biopolymer.

Fig. 2(b) shows the FT-IR spectrum obtained for nanocellulose. It showed the broad peaks at 3332 cm^{-1} attributed to the -OH starching vibrations which involve intramolecular or intermolecular hydrogen bonding in nanocellulose structure. The CH stretching that usually appears at 2900 – 2850 cm^{-1} is not observed for nanocellulose. This might be due to the

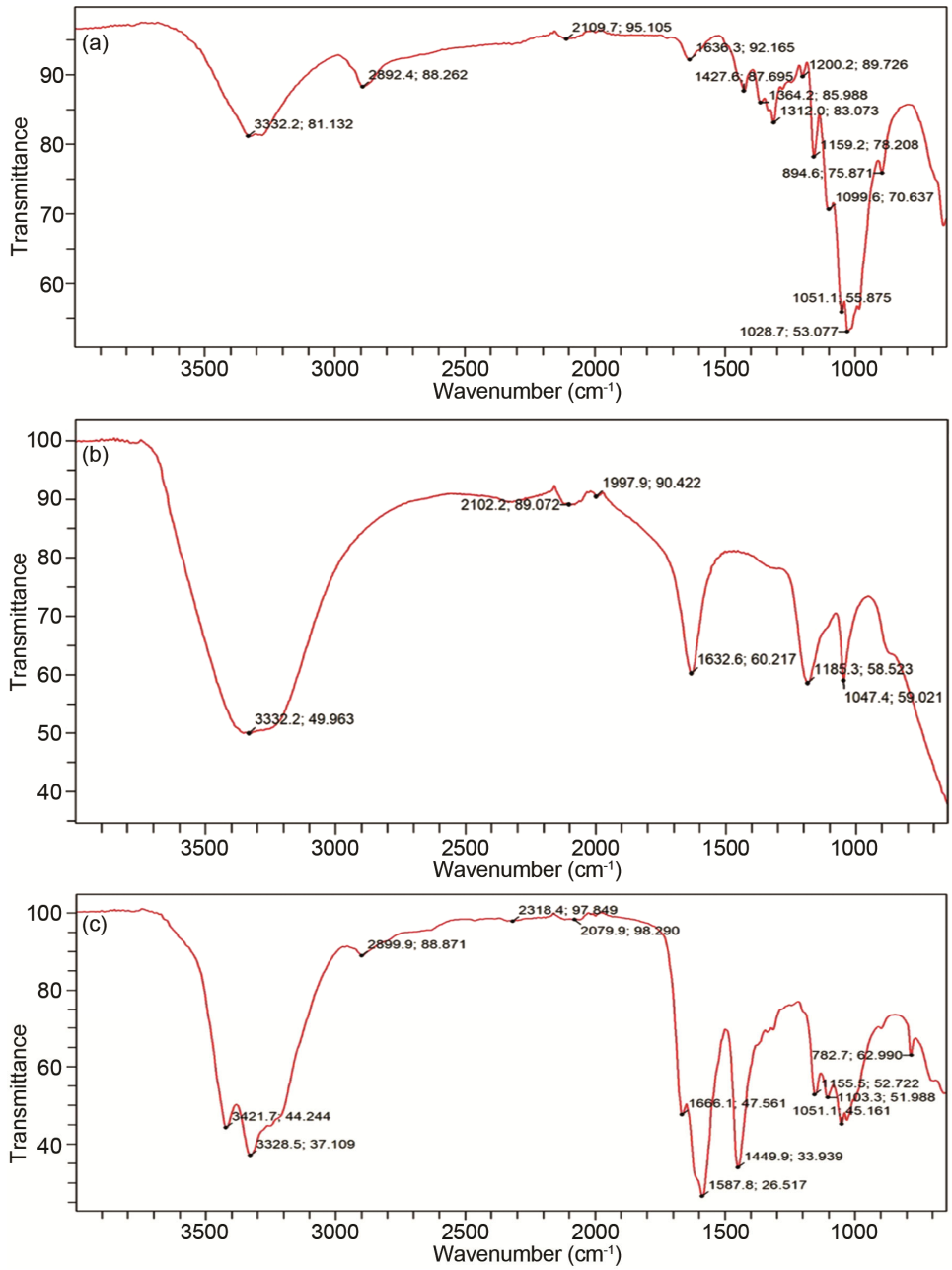

Fig. 2 — FTIR spectra of (a) cellulose, (b) nano cellulose and (c) hydrogel

masking of CH stretching with broad -OH stretching peaks. The strong peak at peak at 1632 cm^{-1} attributes to the -OH bending vibrations. Compared to cellulose sample, the intensity of -OH bending vibrations was relatively high. This might be due to the high water adsorption ability of nanocellulose with high surface area compared to cellulose. Similar to nanocellulose, C-O-C and C-O stretching vibrations were observed at 1185 cm^{-1} and 1047 cm^{-1}, respectively. The peak corresponds to β-glycosidic linkage is not observed due to the disordered molecular arrangement of nanocellulose compared to bulk cellulose leading to overlapping of C-O stretching vibrations with 1047 cm^{-1}. This reveals that the successful formation of nanocellulose without losing the characteristic functionalities of cellulose[45].

The FTIR spectrum of nanocellulose hydrogel is shown in Fig. 2(c). Like cellulose and nanocellulose, this also showed -OH stretching. Unlike cellulose and nanocellulose, the doublet peak was observed in nanocellulose hydrogen at 3421 cm^{-1} and 3328 cm^{-1} which are attributed to -OH stretching bonded via intramolecular hydrogen bonding (O3-H----O5) and that of bonded via intermolecular hydrogen bonding (between OH of adjacent chains). Unlike nanocellulose, C-H stretching vibrations were observed at 2899 cm^{-1} in nanocellulose hydrogel. Peak at 1666 cm^{-1} might be due either -OH bending vibrations or C=O stretching vibrations present in nanocellulose hydrogel. The strong peak at 1587 cm^{-1} was attributed to the asymmetric stretching of $-COO^-$ confirming the presence of deprotonated carboxyl groups. The strong band at 1450 cm^{-1} can be attributed to the symmetric stretching vibration of the carboxylate group ($–COO^-$). This assignment is supported by its characteristic separation of about 170–200 cm^{-1} from the asymmetric $–COO^-$ stretching band observed at 1587 cm^{-1}, which is typical for ionic carboxylate groups. Like cellulose and nanocellulose, it also showed peaks at 1151 cm^{-1} and 1051 cm^{-1} corresponding to C-O-C and C-O stretching vibrations, respectively. The crosslinking and swelling process in hydrogel preparation might disturb the ordered crystalline regions of cellulose and hence the peak corresponding to β-glycosidic linkage is not observed at 897 cm^{-1} as similar to nanocellulose[46]. A band at 783 cm^{-1} is observed which might be due to C-H out of plane bending vibrations. This confirms the successful formation of nanocellulose hydrogel without much affecting the structure of cellulose moieties.

XRD analysis of cellulose, nanocellulose and hydrogel

The XRD pattern of cellulose as shown in Fig. 3(a), displays distinct reflections typical of semi-crystalline cellulose. A sharp and intense diffraction peak located at $2\theta = 22.6°$ corresponds to the (200) crystallographic plane of cellulose I, which is associated with the highly ordered parallel chain alignment along the crystalline axis. Additional broad peaks appearing between $2\theta = 16°$ and 18° correspond to the (1–10) and (110) planes, representing the amorphous and less ordered domains arising from disoriented cellulose chains.The combination of a dominant sharp (200) reflection with overlapping broad (1–10) and (110) peaks indicate the coexistence of crystalline and amorphous regions characteristic of native or regenerated cellulose. The interplanar spacing (d-spacing) of the principal (200) plane, calculated from Bragg's law ($n\lambda=2d\sin\theta$), is 1.958 Å, which closely matches the cellulose I lattice parameters reported in literature, confirming the structural identity of the sample. The degree of crystallinity, qualitatively estimated from the intensity ratio of the crystalline (200) peak at 22.6° to the amorphous background near 18°, reveals a moderate-to-high crystalline fraction[47]. The relatively high peak intensity (≈799 counts) suggests significant molecular ordering in the (200) planes, contributing to enhanced intermolecular hydrogen bonding. Such ordering improves the mechanical strength, dimensional stability, and thermal resistance of the cellulose network.

Fig. 3(b) displays the X-ray diffraction (XRD) pattern of the as-prepared nanocellulose has a diffraction peak at $2\theta \approx 22.5–23.0°$ that corresponds to the (200) crystal plane of cellulose I, which attests to the presence of a semi-crystalline structure. The broad halo observed between 15° and 20° indicates the presence of amorphous zones, suggesting partial disorientation of the native crystalline order of the cellulose after mechanical or chemical treatment. The increased intensity of the (200) peak and reduced amorphous scattering validate that the process of extraction efficiently removed non-cellulosic contents by enhancing the crystalline orientation of cellulose fibrils. The crystallinity index usually reported through the Segal method, is improved over raw cellulose, suggesting improved molecular order at the nanoscale. These outcomes confirm the effective production of high-purity nanocellulose with well-preserved crystalline areas[47,48].

Fig. 3(c) shows the XRD pattern of the hydrogel based on nanocellulose has two clear diffraction peaks located around 2θ ≈ 15° and 2θ ≈ 22.5°, corresponding to the (1–10) and (200) crystalline planes of cellulose I, respectively. The strong peak at 22.5° indicates the partial retention of the native crystalline structure of cellulose after the formation of the hydrogel. The widening of the peaks seen and the lowering in relative overall intensity compared to pure nanocellulose indicate a loss of crystallinity owing to the inclusion of amorphous polymeric networks and cross-linking agents during hydrogel formation[49]. The breakdown of the ordered domains increases the flexibility and water-holding capacity of the hydrogel matrix. The co-existence of crystalline and amorphous domains shows a perfect structural equilibrium that leads to mechanical stability and reprogrammable swelling behaviour.

SEM analysis of nano cellulose and hydrogel

The SEM micrograph (Fig. 4(a)) of the as-synthesized nanocellulose (at 5.00 KX, SE2 detector, EHT 4.00 kV) shows predominantly elongated platelet-like nanofibrils with well-defined, flat faces

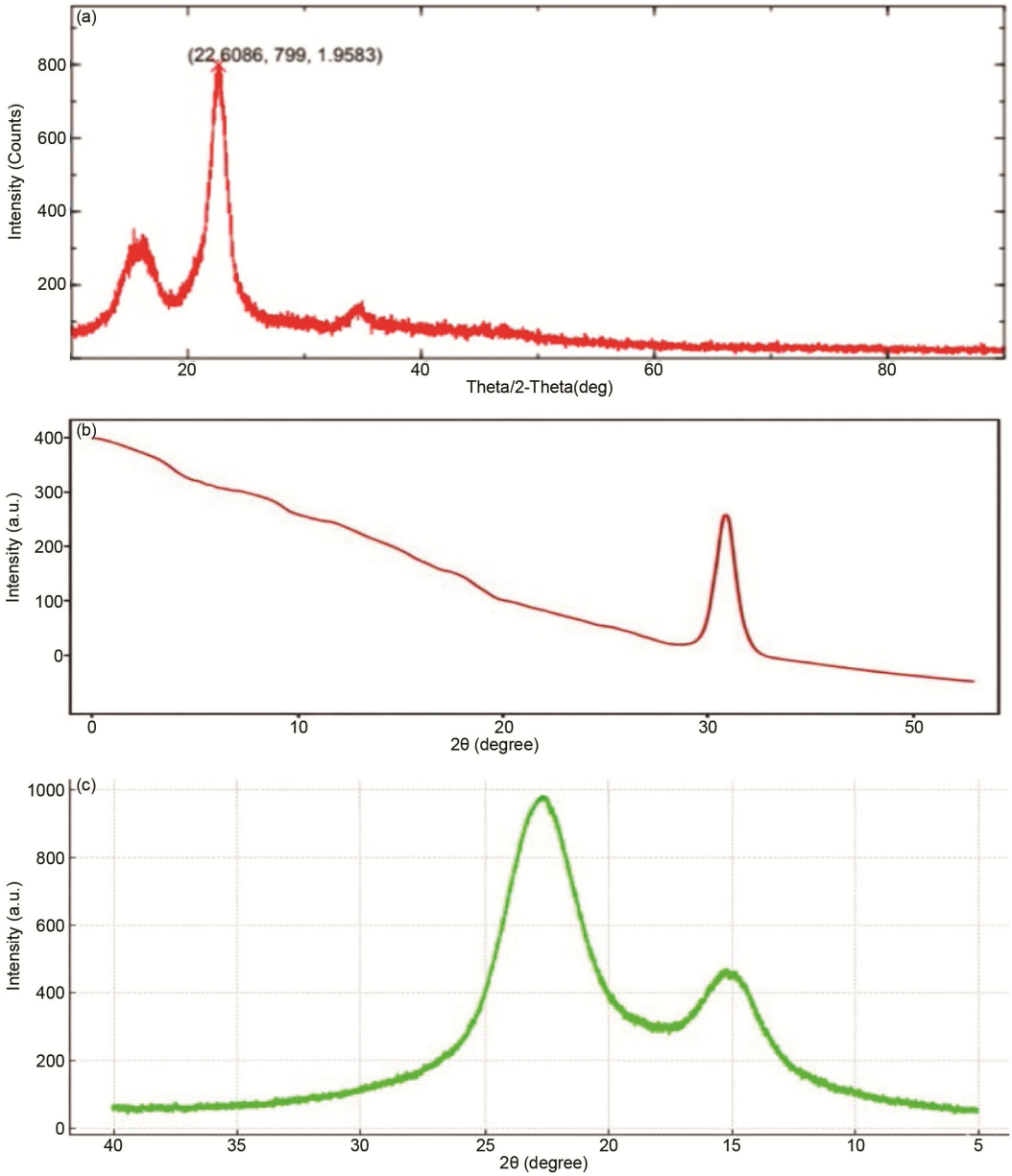

Fig. 3 — X-ray diffractograms of (a) cellulose, (b) nano cellulose and (c) hydrogel

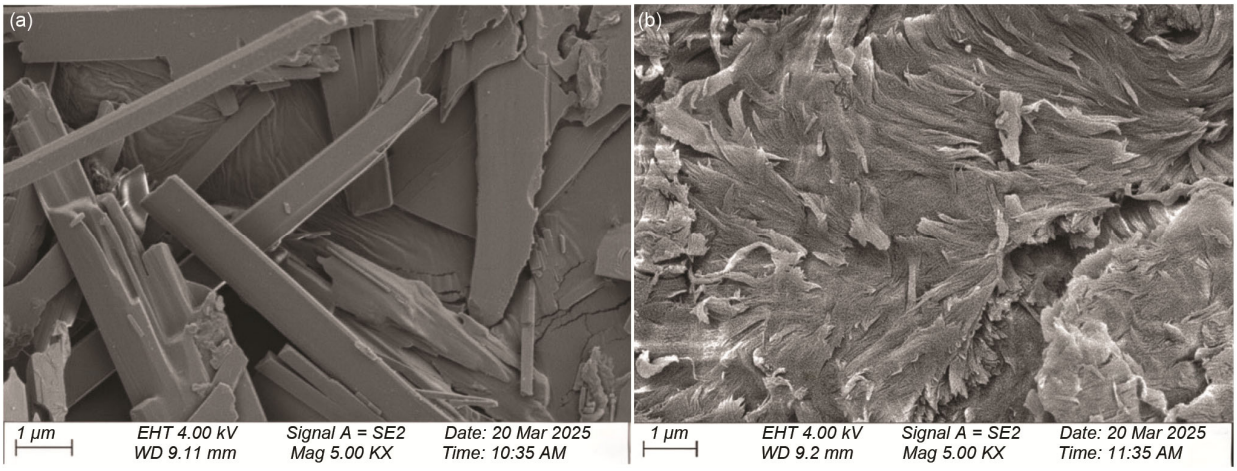

Fig. 4 — SEM micrographs of (a) nano cellulose and (b) hydrogel

and sharp corners. The widths of individual fibrils are in the range ~150–600 nm, while a population of thinner needle-like fragments less than ~200 nm in length exists. The morphology is seen to consist of effective removal of non-cellulosic matrix materials and exposure of crystalline areas, characteristic of short cellulose nanofibers or cellulose nanocrystals derived from chemical isolation. Overlapping, face-to-face stacking and minimal aggregation of the fibrils are indicative of intense inter-fibrillar hydrogen bonding that occurs upon drying. The relatively smooth fibril surfaces and absence of extensive amorphous coatings are conducive to high crystallinity, which is in agreement with XRD results[50]. Damaged ends and platelets likely originate from mechanical damage during processing or sample fracturing. These nanocellulose structures with high aspect ratios are expected to provide outstanding reinforcement ability and high interfacial contact area when incorporated into polymer matrices or hydrogels, enhancing mechanical strength, barrier performance, and network formation critical for hydrogel swelling and load-bearing applications.

The SEM micrograph of nanocellulose hydrogel (Fig. 4(b)), obtained at 5.00 KX magnification under 4.00 kV accelerating voltage, indicates a well-defined three-dimensional, porous, and networked fibrous structure. Layered, sheet-like structures with nanoscale fibrils interconnecting them are found on the hydrogel surface, indicating the uniform distribution of nanocellulose throughout the hydrogel matrix. The ridged and folded surface texture of the morphology under observation is a result of the hydrogen-bonded network formed between nanocellulose fibrils and polymeric chains, suggesting very good interfacial compatibility and effective cross-linking during gelation.

The porous microstructure of submicron size enables high nutrient exchange, ion diffusion, and water retention important to ensure hydrogel functionality in agriculture and medicine. Compared to the SEM nanostructure of unpurified nanocellulose, hydrogel shows a change from rod-like rigid fibrils to a close network with no pores, indicating successful hydrogel formation through partial reorganization of crystalline regions of nanocellulose and association with amorphous domains[51]. The close fibrillar intercontact indicates an enhanced mechanical stability and toughness, which is crucial for multiple swelling-deswelling cycles.

Overall, SEM morphology confirms that nanocellulose is an excellent reinforcing and cross-linking scaffold that imparts hierarchical structuring, increased stability, and homogeneity to the hydrogel matrix. Such structural features correlate with the hydrogel's improved mechanical integrity, water absorption, and functional viability, consistent with XRD confirmation of retained semi-crystallinity and FTIR evidence of hydrogen bonding interactions.While direct swelling ratio measurements were not initially included, the discussion has now been strengthened by correlating SEM-observed porous structure and XRD-revealed partial amorphous characteristics with expected swelling behaviour.

The percentage increase in water retention was determined by comparing the water holding capacity of untreated soil (baseline: 50%) with hydrogel-treated soil, calculated using the following equation and the results are shown in Table 2.

Table 2 — Soil test parameters after hydrogel application

S. No	Parameters	Unit	Test method	Results
1	Water content	%	IS 2720-2[23]	12.4
2	Available phosphorous	µg/g	SOP No. Soil/001[28]	21
3	Ammoniacal nitrogen	mg/kg	IS 14684:1999[36]	7.6
4	Total Kjeldahl nitrogen	%	IS 14684:1999[36]	13.1
5	Water holding capacity	%	SOP No. Soil/011[37]	39
6	Soluble sodium	mg/kg	FAO Method[41]	1951
7	Soluble potassium	mg/kg	FAO Method[42]	104

Table 3 — Comparative evaluation of cellulose-based hydrogel with present study

Material name	Water holding capacity (%)	Nutrient release efficiency (%)	Biodegradability (days)	Outcomes	Reference
Coconut shell-derived nanocellulose hydrogel (Present study)	50	88	60	Enhanced soil moisture retention, slow urea release, improved total nitrogen (13.1%), eco-friendly and scalable	Present study
TEMPO-oxidized cellulose nanofiber hydrogel	48	80	50	High porosity, improved nutrient and water transport, rapid biodegradation	4
Wheat straw nanocellulose hydrogel	46	75	55	Improved swelling capacity and gradual nutrient diffusion	5
Cellulose nanofibril hydrogel crosslinked with citric acid	43	81	65	Biodegradable, stable water uptake, improved soil texture	6
Microcrystalline cellulose–chitosan hydrogel	41	70	80	Good mechanical stability, slower biodegradation, suitable for controlled fertilizer release	9
Nanocellulose–poly(acrylic acid) superabsorbent hydrogel	60	85	90	Superior swelling, extended nutrient release period, less biodegradable	13
Nanocellulose–starch blend hydrogel	47	73	65	Eco-friendly, moderately stable structure, suitable for agricultural field trials	14
Bamboo cellulose hydrogel	49	82	68	Excellent mechanical integrity, efficient soil water retention	22
Cotton linter nanocellulose aerogel hydrogel	52	86	75	High swelling ratio, faster urea diffusion, renewable feedstock	44
Jute-fiber nanocellulose hydrogel	45	79	60	Retained crystalline cellulose I structure, moderate release kinetics	52

$$\text{Water retention increase (\%)} = \left(\frac{W_t - W_0}{W_t}\right) \times 100$$

where W_t is the water retention after treatment and W_o is the initial soil water retention

When comapred with the unreated soil, 50% improvement in water retention capacity compared to untreated soilwas observed for the nano cellulose-based hydrogel. Soil analysis after application revealed a substantial increase in nutrient availability, with ammoniacal nitrogen reaching 7.6 mg/kg and total Kjeldahl nitrogen increasing to 13.1%, confirming improved nutrient retention. The present results of water holding capacity, nutrient release efficiency and biodegradibility are compared with the reported literature and shown in Table 3.

Conclusion

The present study successfully developed a nanocellulose-based hydrogel from coconut shell waste and demonstrated its effectiveness as a sustainable material for agricultural applications. The synthesized hydrogel exhibited a well-defined porous and interconnected network structure, as confirmed by SEM analysis, while FTIR results verified successful crosslinking through the formation of carboxylate groups. XRD analysis further indicated partial retention of cellulose crystalline structure with increased amorphous regions that contributed to enhanced swelling and water absorption characteristics. Besides, the synthesized hydrogel showed a significant improvement in soil performance, achieving 50% improvement in water retention capacity compared to untreated soil. Soil analysis after application revealed a substantial increase in nutrient availability, with ammoniacal nitrogen reaching 7.6 mg/kg and total Kjeldahl nitrogen increasing to 13.1%, confirming improved

nutrient retention. Overall, this study provides a viable approach for converting agricultural waste into a high-value functional material. The developed hydrogel offers a solution for water management and nutrient delivery, making it a promising candidate for sustainable and climate-resilient agricultural practices.

Acknowledgements

The authors thanks to the management of Hindusthan Educational trust for providing a facility.

Conflict of Interest

The authors declare no conflict of interest.

References

1 Poulose A, Parameswaranpillai J, George J J, Gopi J A, Krishnasamy S, Midhun D C D, Hameed N, Salim N V, Radoor S & Sienkiewicz N, Nanocellulose: A fundamental material for science and technology applications, *Molecules*, 27 (2022) 8032.

2 Habibi Y, Lucia L A & Rojas O J, Cellulose nanocrystals: Chemistry, self-assembly, and applications, *Chem Rev*, 110 (2010) 3479.

3 Klemm D, Philipp B, Heinze T, Wagenknecht U & Fischer S, Comprehensive cellulose chemistry: Functionalization of cellulose, *Prog Polym Sci*, 26 (1998) 1529.

4 Isogai A, Saito T & Fukuzumi H, TEMPO-oxidized cellulose nanofibers, *Polym J*, 43 (2011) 213.

5 Alemdar A & Sain M, Isolation and characterization of nanofibers from agricultural residues-wheat straw and soy hulls, *Bioresour Technol*, 99 (2008) 1664

6 Contreras-López O M, Rodríguez-Morales J A & Zuluaga R, Nanocellulose hydrogels: recent advances in their preparation, properties, and applications, *Nanomaterials*, 10 (2020) 108.

7 Nechyporchuk O, Belgacem M N & Bras J, Production of cellulose nanofibrils: A review of recent advances, *Carbohydr Polym*, 157 (2017) 407.

8 Moon R J, Schueneman G & Xu H, Cellulose nanomaterials as chiral templates, *MRS Bull*, 41 (2012) 291.

9 Liu A, Liu J & Yao F, Superabsorbent polymeric nanocellulose hydrogels: Preparation and properties, *Carbohydr Polym*, 119 (205) 83.

10 Azeredo H M C, Nanocellulose in bio-based food packaging applications, *Ind Crop Prod*, 97 (2017) 664.

11 Belbekhouche S, Bras J, Siqueira G & Sette A M, Water sorption behavior and gas barrier properties of cellulose whiskers and microfibrils films, *Carbohydr Polym*, 83 (2011) 1740.

12 Araki T, Ito O & Tanioka A, Flow properties of microcrystalline cellulose suspension prepared by acid treatment of native cellulose, *Colloids Surf Physicochem Eng Asp*, 142 (1998) 75.

13 Rahimihaghighi M, Gigli M, Ficca V C A & Crestini C, Nanocellulose nanocomposite hydrogels: Technological and environmental issues, *Green Chem*, 20 (2018) 2476.

14 Kalia S, Boufi S, Celli A & Kango S, Nanofibrillated cellulose: Surface modification and properties in starch nanocomposites, *Carbohydr Polym*, 105 (2014) 207.

15 Siró I & Plackett D, Cellulose nanofibrils and microfibrils: An overview of the production, properties, and applications, *Cellulose*, 17 (2014) 459.

16 Dufresne A, Nanocellulose processing and industrial applications, *J Mater Sci*, 53 (2018) 1633.

17 Eichhorn S J, Dufresne A, Aranguren M, Marcovich N E, Capadona J R, Rowan S J, Weder C, Thielemans W, Roman M, Renneckar S, Gindl W, Faruk S, Stine K J, Schieber L & Rånby B, Current international research efforts on cellulose nano-crystals and cellulose nano-fibrils, *J Mater Sci*, 45 (2010) 1.

18 Bellani C, Pollet E, Hebraud A, Pereira F V, Schlatter G, Averous L, Bretas R E S & Branciforti M C, Morphological, thermal, and mechanical properties of poly(ε-caprolactone)/poly(ε-caprolactone)-grafted-cellulose nanocrystals mats produced by electrospinning, *J Appl Polym Sci*, 133 (2016) 43445.

19 Danapriya S, Priya S S, Prasadh S H, Sathish J & Babu N D S G, Extraction of value-added products from marine resources, *Russian J Marine Biol*, 48 (2022) 418.

20 Trache D, Hussin M & Chittur S, Microcrystalline cellulose: Isolation, characterization and suitability for pharmaceutical applications-a review, *Express Polym Lett*, 3 (2016) 726.

21 Jackson J K & O'Neill E A, Biodegradable cellulose hydrogels for tissue engineering applications, *Polymers*, 11 (2019) 1428.

22 Zhao H, Liu S & Zhang J, A review of cellulose-based hydrogels: From preparation to applications, *RSC Adv*, 10 (2019) 16273.

23 BIS "IS 2720-2: Methods of test for soils, Part 2: Determination of water content", Bureau of Indian Standards, Manak Bhawan, Old Delhi, India, (1973).

24 BIS "IS 2720-22: Methods of Test for Soils: Part 22: Determination of Organic Matter (First Revision)", Bureau of Indian Standards, Manak Bhavan, New Delhi, India, (1972).

25 BIS "IS 2720-26: Method of Test for Soils: Part 26 Determination of pH Value (Second Revision)", Bureau of Indian Standards, Manak Bhavan, New Delhi, India, (1987).

26 BIS "IS 14767: 2000 – Determination of the Specific Electrical Conductivity of Soils: Method of Test", Bureau of Indian Standards, Manak Bhavan, New Delhi, India, (2000).

27 EHS360 Labs "SOP No. Soil/010: Standard Operating Procedure for Soil Testing Sulphate", EHS360 Labs, Chennai, India, (2021).

28 EHS360 Labs "SOP No. Soil/001: Standard Operating Procedure Available Phosphorous", EHS360 Labs, Chennai, India, (2021).

29 EHS360 Labs "SOP No. Soil/009: Standard Operating Procedure for Soluble calcium and magnesium", EHS360 Labs, Chennai, India, (2021).

30 EHS360 Labs "SOP No. Soil/008: Standard Operating Procedure for Soluble calcium", EHS360 Labs, Chennai, India, (2021).

31 EHS360 Labs "SOP No. Soil/005: Standard Operating Procedure for Carbonate", EHS360 Labs, Chennai, India, (2021).

32 EHS360 Labs "SOP No. Soil/003: Standard Operating Procedure for Bicarbonate", EHS360 Labs, Chennai, India, (2021).

33 EHS360 Labs "SOP No. Soil/006: Standard Operating Procedure for Chloride", EHS360 Labs, Chennai, India, (2021).

34 EHS360 Labs "SOP No. Soil/004: Standard Operating Procedure for Bulk density", EHS360 Labs, Chennai, India, (2021).

35 EHS360 Labs "SOP No. Soil/007: Standard Operating Procedure for Pore space", EHS360 Labs,Chennai, India, (2021).

36 BIS "IS 14684:1999: Landslide control – Guidelines", Bureau of Indian Standards, Manak Bhawan, New Delhi, India, (1999).

37 EHS360 Labs "SOP No. Soil/011: Standard Operating Procedure for water holding capacity", EHS360 Labs, Chennai, India, (2021).

38 EHS360 Labs "Standard Operating Procedure for FAO Method for soil texture", EHS360Labs, Chennai, India, (2021).

39 EHS360Labs "Standard Operating Procedure for Robinson Pipette Method for sand, slit, clay", EHS360Labs, Chennai, India, (2021).

40 EHS360Labs "Standard Operating Procedure for Inhouse method for Chemical oxygen demand"", EHS360Labs, Chennai, India, (2021).

41 EHS360Labs "Standard Operating Procedure for FAO Method for Soluble sodium", EHS360Labs, Chennai, India, (2021).

42 EHS360Labs "Standard Operating Procedure for FAO Method for Soluble pottasium", EHS360Labs, Chennai, India, (2021).

43 EHS360Labs "Standard Operating Procedure for FAO Method for Cation exchange capacity", EHS360Labs, Chennai, India, (2021).

44 Dufresne A, Cellulose nanomaterials as biobased macromolecular materials, *Macromolecules*, 47 (2018) 4111.

45 Sathish J & Palani R, Development and characterization of chitin-based hydrogel nanocomposites from animal shells for sustainable agriculture, *Periodica Polytechnica Chem Eng*, 69 (2025) 480.

46 Zhang J & Lu C, Nanocellulose hydrogels as scaffolds for tissue engineering, *Biomaterials*, 103 (2016) 20.

47 Babu N D S G, Ponnam V & Tondepu S, Synthesis of magnesium titanate from magnesium chloride a byproduct of zirconium plant, *J Sustain Metall*, 11 (2025) 2561.

48 Sathish J & Palani R, Development and characterization of chitin-based hydrogel nanocomposites from animal shells for sustainable agriculture, *Periodica Polytechnica Chem Eng*, 69 (2025) 480.

49 Ureña-Benavides E E & Gnanasekharan V, Review on the properties and applications of cellulose nanocrystals, *J Nanomater*, 2015 (2016) 616053.

50 Babu N S G, Ponnam V, Tondepu S & Shanmugapriya S P, Enhanced catalytic pyrolysis for sustainable transformation of waste plastics into energy resources, *J Inst Eng (India): Ser D*, 106 (2025) 483.

51 Sehaqui H & Zhou Q, Super-absorbent, super-adsorbent, and super-flexible: Aerogels from nanocellulose, *Soft Matter*, 7 (2017) 8752.

52 Zhu H & Fang Z, Nanocellulose-based hydrogels: Synthesis, properties, and applications, *ACS Nano*, 10 (2022) 621.